HHS Public Access

Author manuscript

Respir Physiol Neurobiol. Author manuscript; available in PMC 2018 December 01.

Published in final edited form as:

Respir Physiol Neurobiol. 2017 December ; 246: 39–46. doi:10.1016/j.resp.2017.07.007.

Compensatory Effects Following Unilateral Diaphragm Paralysis

Obaid U. Khurram[a], **Gary C. Sieck**[a,b], and **Carlos B. Mantilla**[a,b,*]

[a]Departments of Physiology & Biomedical Engineering, Mayo Clinic, Rochester, MN 55905

[b]Departments of Anesthesiology and Perioperative Medicine, Mayo Clinic, Rochester, MN 55905

Abstract

Injury to nerves innervating respiratory muscles such as the diaphragm muscle results in significant respiratory compromise. Electromyography (EMG) and transdiaphragmatic pressure (Pdi) measurements reflect diaphragm activation and force generation. Immediately after unilateral diaphragm denervation (DNV), ventilatory behaviors can be accomplished without impairment, but Pdi generated during higher force non-ventilatory behaviors is significantly decreased. We hypothesized that 1) the initial reduction in Pdi during higher force behaviors after DNV is ameliorated after 14 days, and 2) changes in Pdi over time after DNV are associated with concordant changes in contralateral diaphragm EMG activity and ventilatory parameters. In adult male rats, the reduced Pdi during occlusion (~40% immediately after DNV) was ameliorated to ~20% reduction after 14 days. Contralateral diaphragm EMG activity did not significantly change immediately or 14 days after DNV compared to the pre-injury baseline for any motor behavior. Taken together, these results suggest that over time after DNV compensatory changes in inspiratory related muscle activation may partially restore the ability to generate Pdi during higher force behaviors.

1. Introduction

The final common pathway of neuromotor control is the motor unit, which consists of an α-motoneuron and the group of muscle fibers it innervates (Liddell et al., 1925). Recruitment of additional motor units (Fournier et al., 1988; Sieck, 1988; Sieck et al., 1989) and/or an increase in the discharge frequency of recruited motor units (Fournier et al., 1988; Iscoe et al., 1976; Seven et al., 2014; Sieck et al., 1984) increase the force generated by skeletal muscles including respiratory muscles such as the diaphragm. Indeed, orderly recruitment of diaphragm motor units allows for a broad range of motor behaviors from lower force ventilatory behaviors (requiring only 10 – 30% of the total force generating capacity of the diaphragm across species) and less frequent higher force behaviors that are necessary for maintaining airway patency (e.g. coughing, sneezing, sighing) (Mantilla et al., 2014; Mantilla et al., 2010; Sieck et al., 1989). While recruitment of only fatigue resistant motor

Mary Brigh 2-752, St Marys Hospital, Mayo Clinic, 200 First St SW, Rochester, MN 55905. Tel.: +(507) 255-7481; Fax: +(507) 255-7300. mantilla.carlos@mayo.edu.

units is sufficient to accomplish lower force ventilatory behaviors, recruitment of more fatigable motor unit types is necessary to accomplish higher force behaviors (Mantilla et al., 2010; Mantilla et al., 2011b; Sieck, 1991; Sieck, 1994; Sieck et al., 1989). This large reserve capacity for force generation by the diaphragm muscle results in the ability to sustain ventilatory behaviors despite substantial loss of motor units (Alvarez-Argote et al., 2016; Gill et al., 2015; Mantilla et al., 2011b; Rana et al., 2016).

Unilateral phrenic nerve denervation (DNV) induces unilateral diaphragm paralysis, effectively inactivating 50% of the motor unit output of the diaphragm (Miyata et al., 1995; Zhan et al., 1995). We previously showed that immediately after unilateral DNV, transdiaphragmatic pressure (Pdi; an indirect measure of diaphragm force) decreases for behaviors requiring greater than 50% of the maximal Pdi in rats (Gill et al., 2015). In the same study, we showed that Pdi amplitude during ventilatory behaviors is unimpaired after DNV and ventilation is unimpaired as assessed by blood gas levels. Similarly, in humans, while maximal Pdi amplitude is reduced after unilateral diaphragm paralysis, Pdi amplitude necessary to accomplish quiet breathing (eupnea) is generally unimpaired although relative contributions from the gastric and esophageal components of Pdi may change (Hart et al., 2002; Hillman et al., 1988; Lisboa et al., 1986). In dogs, Pdi measurements across respiratory motor behaviors after unilateral diaphragm paralysis is not available, but there is some evidence that tidal volume does not change following unilateral diaphragm paralysis (Katagiri et al., 1994) and thus impairment in Pdi during eupnea is unlikely. Accordingly, the purpose of the present study was to determine whether compensation for reduced Pdi during higher force behaviors occurs over a period of 14 days in rats, and the role of the contralateral diaphragm muscle in this compensation. We hypothesized that 1) the initial reduction in Pdi during higher force behaviors after DNV is ameliorated after 14 days, and 2) changes in Pdi over time post-DNV are associated with concordant changes in contralateral diaphragm electromyographic (EMG) activity and ventilatory parameters.

2. Materials and methods

1.1. Animals

All experiments were approved by the Institutional Animal Care and Use Committee of the Mayo Clinic. A total of 29 adult, male Sprague-Dawley rats (280–380 g) from Envigo (Indianapolis, IN) were used for this study. Anesthesia was achieved via intramuscular injections of ketamine (100 mg/kg) and xylazine (10 mg/kg) for all surgical procedures, Pdi and EMG recordings. Unilateral diaphragm paralysis was verified by the absence of EMG activity in the ipsilateral (right) diaphragm at all time points in the DNV group (n = 14). Control rats did not receive either DNV or exposure of the phrenic nerve (n = 15).

2.2. Unilateral diaphragm denervation

The right phrenic nerve was isolated in the lower neck and a 10–20 mm length of the nerve was sectioned as previously described (Geiger et al., 2003; Gill et al., 2015; Gosselin et al., 1994; Miyata et al., 1995; Zhan et al., 1995; Zhan et al., 1997; Zhan et al., 1992). Briefly, rats were laid in a supine position and a 2 cm incision was made starting from the middle of the clavicle in a rostromedial direction. Blunt dissection was performed to isolate the phrenic

nerve, using the jugular vein, carotid artery, and brachial plexus as anatomical landmarks. Complete DNV was verified by absence of EMG activity in the ipsilateral hemidiaphragm.

2.3. Transdiaphragmatic pressure measurements

Pdi was calculated as the difference in pressures measured between esophageal (P_{eso}) and gastric (P_{ab}) catheters as previously described (Gill et al., 2015; Greising et al., 2013a; Greising et al., 2013b; Mantilla et al., 2010; Sieck et al., 1989). Briefly, two 3.5 French Millar solid-state pressure catheters (SPR-524; Millar Instruments, Houston, TX) were inserted through the mouth into the esophagus and stomach. Correct catheter position was determined based on the direction of signal deflection during real-time measurements. Intra-thoracic and abdominal pressures were recorded and digitized (400 Hz) with PowerLab 4/35 and visualized in real-time with LabChart 8 (ADInstruments, Colorado Springs, CO). The Pdi signal was band-pass filtered between 0.3 and 30 Hz using a digital filter to remove offset and high-frequency noise. Data were exported for *post hoc* analysis using a custom-designed semi-automated script in MATLAB (MathWorks, Natick, MA). Peak amplitude, both instantaneous and average respiratory rate, inspiratory duration, and duty cycle were determined using previously described techniques (Medina-Martinez et al., 2015). Pdi measurements across all motor behaviors were obtained before, immediately after, and 14 days after unilateral DNV in the DNV group; in the time control group, measurements were made at two time points separated by 14 days. The abdomen was bound during Pdi measurements to approximate isometric conditions during diaphragm muscle contraction.

2.4. Diaphragm EMG measurements

Diaphragm EMG was recorded using chronically placed wire electrodes as previously described (Dow et al., 2006; Dow et al., 2009; Mantilla et al., 2011a; Trelease et al., 1982). Briefly, pairs of multistranded fine wire stainless steel electrodes (AS631; Cooner Wire Inc., Chatsworth, CA) were stripped to expose an ~2 mm segment. A laparotomy was performed and a pair of electrodes with the exposed portion of the wire implanted into the mid-costal regions of both sides of the diaphragm with an inter-electrode distance of ~3 mm. The electrodes were tunneled and externalized in the dorsum of the animals for up to 19 days. Electrode implantation was performed 4 days prior to DNV. The ends of the fine-wire electrodes were connected via gold pin connectors to differential amplifiers (Model EMG100C, Biopac Systems Inc., Goleta, CA.). The EMG signal was amplified (2000x), band-pass filtered (100–5000 Hz) and digitally sampled at 10 kHz using Powerlab 4/35. During each recording session, the ECG signal present in the diaphragm EMG signal was isolated using a low-pass digital filter (f_c = 200 Hz) in LabChart 8 and used to determine the instantaneous heart rate.

Data were exported to MATLAB, downsampled to 2000 Hz, and analyzed using custom-made software based on previous work (Dow et al., 2006). For diaphragm EMG recordings, ECG contamination was removed by linearly correlating the average ECG tracing of each signal against each set of points within the signal. A threshold was set manually such that a cross correlation at a set of points greater than this threshold resulted in subtraction of the average ECG. The root mean square (RMS) of the EMG signal was calculated with a 50 ms window. The peak of the RMS EMG (RMS_{peak}) and central respiratory drive, estimated by

measuring the RMS EMG value at 75 ms after the onset of activity (RMS_{75}), were determined for each behavior and time (Gill et al., 2015; Seven et al., 2014). All RMS EMG measurements were normalized to the pre-injury sigh RMS_{peak} for each animal. We have previously demonstrated that normalizing RMS values to near maximal behaviors such as sigh and sneeze reduces inter-animal variability over time (Mantilla et al., 2011a). In addition, the tension-time index of the diaphragm was used as estimate of the efficiency of diaphragm activation before, immediately after, and 14 days after DNV was derived from the Pdi and EMG (Bellemare et al., 1982). The tension-time index was calculated as Pdi amplitude (normalized to Pdi_{max}) * Duty Cycle (Bellemare et al., 1982). For this estimate, Pdi_{max} at each time point was assumed to be 37 cm H_2O before and 23 cm H_2O after DNV, as previously reported (Gill et al., 2015; Mantilla et al., 2010).

2.5 Motor behaviors

Data were collected during 1) breathing of room air (eupnea), 2) exposure to hypoxia (10% O_2)-hypercapnia (5% CO_2), 3) deep breaths ("sighs", defined as spontaneously occurring inspiratory events that were greater than 2 times eupneic Pdi amplitude at the baseline) and 4) sustained airway occlusion for ~45 s, as in previous studies (Mantilla et al., 2011a; Mantilla et al., 2010; Seven et al., 2014). Rats were given sufficient time between behaviors to allow for acclimatization to normal breathing as determined by real-time calculation of Pdi amplitude and respiratory rate. For both eupnea and hypoxia-hypercapnia, 20 representative breaths that were uncontaminated by ECG, were selected to determine the RMS_{peak} and RMS_{75}. For airway occlusion, the 5 largest breaths within the last 10 s of the occlusion period were analyzed, as in previous studies (Gill et al., 2015; Mantilla et al., 2010; Seven et al., 2014).

2.6. Statistics

All statistical evaluations were performed using standard statistical software (JMP Pro 11, SAS Institute Inc., Cary, NC). Differences in Pdi, sigh normalized diaphragm EMG activity, and ventilatory parameters across experimental groups and motor behaviors were evaluated using a mixed linear model with behavior (eupnea, hypoxia-hypercapnia, sigh, occlusion), time (baseline, immediately after denervation, and 14 days afterwards), and the behavior*time interaction as fixed effects and with animal number as a random effect. When appropriate, *post hoc* analyses were conducted using the Tukey-Kramer Honestly Significant Difference (HSD) test, unless otherwise noted. Statistical significance was established at $p < 0.05$. A subset of rats were not included in the final analysis due to inability to chronically monitor EMG activity (n = 6; e.g., resulting from electrode dislodgement) or based on *a priori* criteria on the proportional Pdi amplitude at baseline during eupnea compared to sighs (n = 6; sighs must be greater than 2 times the eupneic amplitude). All experimental data are presented as mean ± standard error (SE) across animals, unless otherwise specified.

3. Results

A total of 29 animals were successfully bilaterally implanted with EMG electrodes in the midcostal diaphragm for chronic EMG recordings. All animals tolerated implantation of electrodes without changes in ventilation suggestive of pneumothorax or requirement for

mechanical ventilation. At the baseline, there were no significant differences in Pdi amplitude during eupnea (~9 cm H_2O) or any other respiratory parameter between animals included in the chronic EMG analyses (n = 17) and those that were not (n = 12). A total of 9 (out of 17) animals received a phrenic nerve transection (DNV group) and 8 received no further surgery (control group). Representative tracings of EMG, RMS EMG, and Pdi generated during ventilatory and non-ventilatory motor behaviors are shown in Fig. 1. All of the data shown are from a single representative animal from the DNV group. During each recording session, anesthetic depth was kept consistent across animals by continuous monitoring of heart rate and respiratory frequency as well as frequent visual inspection of the toe pinch response and palpebral reflex.

3.1. Transdiaphragmatic pressure (Pdi) measurements

Pdi amplitude was successfully recorded at baseline, immediately after unilateral DNV, and 14 days afterwards in all 11 animals. Average Pdi amplitudes across all behaviors and at each time are shown in Fig. 2. In the control group, the mixed linear model revealed significant differences in Pdi amplitude across behaviors ($F_{3,48} = 98$, $p < 0.001$), but not time ($F_{1,48} = 1$, p = 0.715) or the interaction of behavior and time ($F_{3,48} = 1$, p = 0.528). During both eupnea and hypoxia-hypercapnia, Pdi was consistent over time. Averaged across all time points, the coefficient of variation in Pdi during both eupnea and hypoxia-hypercapnia was 6% in the control group and 7% and 6%, respectively, in the DNV group. Pdi amplitude was ~2- and 4-fold greater than eupneic Pdi during sighs and occlusion, respectively. No significant differences in Pdi were found between eupnea and hypoxia-hypercapnia. In the DNV group, significant effects on Pdi amplitude across behaviors ($F_{3,87} = 156$, $p < 0.001$), time ($F_{2,87} = 20$, $p < 0.001$), and the interaction of behavior and time ($F_{6,87} = 6$, $p < 0.001$) were evident. Pdi was significantly greater at the pre-injury baseline compared to Pdi immediately after and 14 days after DNV. In addition, 14 days after DNV, Pdi was significantly greater than immediately after DNV indicating partial recovery. During eupnea and hypoxia-hypercapnia, Pdi was unaffected after DNV compared to the pre-injury baseline and remained unchanged 14 days after DNV. In contrast, Pdi generated during both sighs and airway occlusion was reduced significantly after DNV. Compared to the pre-injury baseline of ~21 cm H_2O for sighs, Pdi generated during sighs was significantly reduced to ~14 cm H_2O immediately after DNV. By 14 days after DNV, this 35% reduction in Pdi during sigh was ameliorated to a 20% reduction (~17 cm H_2O), and the differences in Pdi were no longer statistically significant compared to either the pre-injury baseline or immediately after DNV. Pdi generation during airway occlusion followed a similar trend, but was significantly reduced from a pre-injury value of ~31 cm H_2O down to ~20 cm H_2O immediately after DNV. This 40% reduction in Pdi was ameliorated to a 20% reduction (~27 cm H_2O) by 14 days after DNV. At this terminal time point, Pdi during occlusion was significantly different from both the pre-injury baseline as well as the Pdi immediately after DNV. Additionally, in order to assess whether recovery of Pdi over time was primarily due to a change in esophageal or gastric pressures we plotted Pes vs Pga across behaviors before, immediately after, and 14 days after DNV. The slope of this relationship generally reflects the relative contributions of the chest wall inspiratory muscles and diaphragm to Pdi. Accordingly, a linear regression was performed for each animal across motor behaviors at each time point and the average slope and y-intercept across animals were determined for

each time point. The average slopes across animals were 4.6 ± 5.7, 5.4 ± 1.1, and 5.6 ± 3.0 before, immediately after, and 14 days after DNV, respectively. No significant differences in slope were evident between time points ($p \geq 0.881$ for all pairwise comparisons), consistent with the relative contributions of the diaphragm and chest wall inspiratory muscles to Pdi being preserved over time post-DNV.

3.2. Diaphragm peak RMS EMG amplitude (RMS_{peak})

All EMG recordings were obtained simultaneously with Pdi measurements. Diaphragm RMS_{peak} values across all behaviors and at each time are shown in Fig. 3. In the control group, the mixed linear model revealed significant differences in RMS_{peak} across behaviors ($F_{3,48} = 26$, $p < 0.001$) and time ($F_{1,48} = 8$, $p = 0.005$), but not of the interaction of behavior and time ($F_{3,48} = 1$, $p = 0.574$). RMS_{peak} during both airway occlusion and sighs was ~2–3 times greater than RMS_{peak} during eupnea (43 ± 3%) and hypoxia-hypercapnia (47 ± 2%). No significant differences in RMS_{peak} were found during eupnea and hypoxia-hypercapnia. In uninjured control animals, RMS_{peak} 14 days after baseline was significantly greater than RMS_{peak} at the baseline and this trend was consistent within each behavior. These results reflect increased RMS EMG activity without any intervention over a period of 14 days, consistent with previous results (Mantilla et al., 2011b). In the DNV group, significant effects on RMS_{peak} across behaviors ($F_{3,87} = 91$, $p < 0.001$) and time ($F_{2,87} = 5$, $p = 0.011$), but not of the interaction between behavior and time ($F_{6,55} = 1$, $p = 0.304$), were evident. RMS_{peak} increased significantly by 14 days after DNV compared to the baseline, but not compared to immediately after DNV. There were no statistically significant differences in RMS_{peak} immediately after DNV compared to the baseline. In order to further discriminate whether increases in RMS_{peak} over time varied between groups, an additional mixed linear model with behavior, time (restricted to baseline and 14 days later), group (control and DNV), and the behavior*time, group*time, group*behavior, and group*time*behavior interactions was performed. This mixed linear model revealed a significant effect on RMS_{peak} of both behavior ($F_{3,103} = 74$, $p < 0.001$) and time ($F_{1,103} = 16$, $p < 0.001$). Importantly, there were no significant effects on RMS_{peak} of group ($F_{1,15} = 1$, $p = 0.947$) or the interaction between group and time ($F_{1,103} = 1$, $p = 0.339$). Additionally, the model revealed no significant effects of behavior*time ($F_{3,103} = 2$, $p = 0.110$), group*behavior ($F_{3,103} = 1$, $p = 0.913$), and group*time*behavior ($F_{3,103} = 1$, $p = 0.866$). These findings are consistent with a lack of evidence for an effect of DNV on diaphragm RMS_{peak}.

3.3. Estimated central respiratory drive (RMS_{75})

Neural drive to phrenic motoneurons (central respiratory drive) was estimated by RMS_{75} (normalized RMS value at 75 ms after onset of activity) as previously described (Gill et al., 2015; Seven et al., 2014). RMS_{75} across all behaviors and at each time are plotted in Fig. 4. In the control group, the mixed linear model revealed a significant difference in RMS_{75} across behaviors ($F_{3,48} = 12$, $p < 0.001$), but not time ($F_{1,48} = 2$, $p = 0.218$) or the interaction of behavior and time ($F_{3,48} = 1$, $p = 0.977$). RMS_{75} during airway occlusion was ~2 times the RMS_{75} during eupnea, hypoxia-hypercapnia, and sigh, all of which were not significantly different from one another. In the DNV group, there was a significant effect on RMS_{75} across behaviors ($F_{3,87} = 41$, $p < 0.001$), but not time ($F_{2,87} = 3$, $p = 0.055$) or the

interaction of behavior and time ($F_{2,87} = 2$, $p = 0.181$), consistent with no evidence for an effect of DNV on RMS_{75}.

3.4 Ventilatory Parameters

Table 1 shows ventilatory parameters determined from Pdi signals and includes respiratory rate, inspiratory duration, duty cycle, and the tension-time index for both control and DNV groups. Respiratory rate, inspiratory duration, and duty cycle were obtained by semi-automated analysis of the Pdi signal for each animal (Medina-Martinez et al., 2015), while the tension-time index was calculated as described in the Materials & Methods.

In the control group, the mixed linear model revealed significant differences in respiratory rate ($F_{1,21} = 39$, $p < 0.001$) and duty cycle ($F_{1,21} = 23$, $p < 0.001$), but not inspiratory duration ($F_{1,21} = 1$, $p = 0.290$) across ventilatory behaviors. There were no effects of time or behavior*time interaction on any of these respiratory parameters ($p \geq 0.230$ and $p \geq 0.483$, respectively). In the DNV group, significant effects of behavior and time on respiratory rate ($F_{1,40} = 58$, $p < 0.001$ and $F_{2,40} = 11$, $p < 0.001$, respectively) and duty cycle ($F_{2,40} = 52$, $p < 0.001$ and $F_{2,40} = 17$, $p = 0.030$, respectively) were observed. There was a significant difference in inspiratory duration of time ($F_{2,40} = 73$, $p < 0.001$), but not behavior ($F_{1,40} = 1$, $p = 0.525$). There was no behavior*time interaction on any of these respiratory parameters ($p \geq 0.665$).

Respiratory rate was significantly greater during hypoxia-hypercapnia compared to eupnea in both the control and DNV groups (~30% increase), as expected. There was no difference in respiratory rate between baseline measurements and immediately after DNV across behaviors, but there was a significant increase by 14 days after DNV (~15%). In both the control and DNV groups, inspiratory duration during sighs and occlusion was significantly greater than during eupnea and hypoxia-hypercapnia, both of which were not different from each other. Inspiratory duration during ventilatory behaviors increased significantly (~30%) after DNV compared to baseline and returned to baseline by 14 days. Accordingly, duty cycle during hypoxia-hypercapnia was significantly greater than during eupnea in both groups (~20%). Additionally, duty cycle was significantly greater (~20%) immediately after DNV compared to both the pre-injury baseline and 14 days afterwards.

In the control group, the mixed linear model revealed a significant effect on the tension-time index of behavior ($F_{1,21} = 12$, $p = 0.002$), but not time ($F_{1,21} = 1$, $p = 0.138$), or the behavior*time interaction ($F_{1,21} = 1$, $p = 0.930$). The tension-time index was higher during hypoxia-hypercapnia compared to during eupnea, as expected with increased chemical drive. In the DNV group, the mixed linear model revealed a significant effect on the tension-time index of behavior ($F_{1,40} = 32$, $p < 0.001$) and time ($F_{2,40} = 15$, $p < 0.001$), but not the behavior*time interaction ($F_{2,40} = 2$, $p = 0.126$). Similar to the control group, in the DNV group tension-time index during hypoxia-hypercapnia was higher (~50%) than during eupnea. The tension-time index increased significantly after DNV (~60%) and remained elevated above baseline after 14 days (~50%).

4. Discussion

In the present study, Pdi during ventilatory behaviors is unaffected by unilateral DNV even when stimulated by hypoxia-hypercapnia. In contrast, Pdi during higher force non-ventilatory behaviors is reduced by DNV. These results are consistent with our previous observation in rats immediately following DNV (Gill et al., 2015) and generally consistent with studies in dogs and humans (Hart et al., 2002; Hillman et al., 1988; Katagiri et al., 1994; Lisboa et al., 1986). However, the present study examined longer term effects of DNV, extending these previous results by showing that there is partial recovery of ventilatory patterns and the ability to generate Pdi during higher force non-ventilatory behaviors by 14 days after DNV. Inspiratory duration and duty cycle were prolonged immediately after DNV, but returned to baseline by 14 days. Diaphragm RMS_{peak} and RMS_{75} (an estimate of central respiratory drive) were unchanged by DNV during different motor behaviors both immediately and after 14 days. These findings indicate that by 14 days after DNV, compensatory changes in the force generation by inspiratory muscles including the diaphragm partially restore the ability to generate Pdi during higher force behaviors.

4.1. Effect of unilateral DNV on Pdi

There was no evidence of an effect of DNV on Pdi during ventilatory behaviors. The pre-injury baseline Pdi was 8–9 cm H_2O during both eupnea and hypoxia-hypercapnia and remained at this level after DNV. These ventilatory Pdi values are consistent with previously reported values across various species including rats (Gill et al., 2015; Greising et al., 2013b; Mantilla et al., 2010; Sieck, 1991; Sieck, 1994; Sieck et al., 1989; Watchko et al., 1986). In the present study, it was not possible to repeatedly measure maximum Pdi (Pdi_{max}) using bilateral phrenic nerve stimulation, but Pdi_{max} in the rat is 37 cm H_2O (Gill et al., 2015; Mantilla et al., 2010). Accordingly, the Pdi generated during ventilatory behaviors was ~25% of Pdi_{max}. Previously, we reported that immediately after DNV, Pdi_{max} decreased from 37 to 23 cm H_2O (Gill et al., 2015). Thus, the Pdi during ventilatory behaviors immediately after and 14 days after DNV represent a greater fraction of Pdi that can be maximally elicited by the intact hemidiaphragm (~40%). This level of force generation is expected to require the recruitment of additional motor units and/or an increase in the discharge rate of recruited motor units (Mantilla et al., 2011b; Sieck, 1991; Sieck et al., 1989). On the other hand, Pdi amplitude during higher force behaviors (sigh and occlusion) was not maintained after DNV. At baseline, the Pdi generated during sighs was 21 cm H_2O (~55% of Pdi_{max}), in agreement with our previous reports in rats (20–23 cm H_2O) (Gill et al., 2015; Mantilla et al., 2010). Immediately after DNV, Pdi during sighs decreased to 14 cm H_2O, which would still be ~55% of post-DNV Pdi_{max}.

The pre-injury baseline Pdi generated during airway occlusion in the present study was 31 cm H_2O, which is higher than previously reported values of 23 cm H_2O (Gill et al., 2015; Mantilla et al., 2010). In fact, the Pdi value for occlusion observed in the present study approximated the Pdi_{max} previously reported in rats (37 cm H_2O) (Gill et al., 2015; Mantilla et al., 2010). This occlusion Pdi would amount to ~85% of Pdi_{max} compared to ~60% in previous studies. It is possible that this difference is due to the technique used for airway occlusion. In the present study, because of the need to perform repeated measurements, we

employed nasopharyngeal occlusion rather than tracheal occlusion, which may have stimulated trigeminal afferents. Regardless, occlusion Pdi decreased to 20 cmH_2O immediately after DNV and by 14 days after DNV, occlusion Pdi increased to 27 cmH_2O, which would approximate the Pdi that can be maximally elicited by the intact hemidiaphragm (Gill et al., 2015). It is possible that immediately after DNV, the excitability of the phrenic motoneuron pool is suppressed such that there is insufficient recruitment of diaphragm motor units and thus a lower occlusion Pdi. With time, excitability of the phrenic motoneuron pool may be restored allowing near maximal recruitment during airway occlusion. Indeed, in limb muscles subjected to chronic compensatory loading induced by synergist ablation, motoneuron excitability (as measured by the threshold properties of motoneurons) reportedly increased over time (Krutki et al., 2015). In the case of the diaphragm muscle, both hemidiaphragms are activated synchronously and are synergistic during ventilatory behaviors (De Troyer et al., 2003). However, motor unit properties show inconsistent responses to injury that may reflect at least in part the time post-injury and the injury model itself (Baltina et al., 2006; Harvey et al., 2006; Thomas et al., 2016; Tissenbaum et al., 1991). Future studies are needed to elucidate the contribution of motor units in the intact hemidiaphragm and the impact of motoneuron axotomy on the properties of motor units in synergist muscles. Another possibility is that other respiratory muscles (e.g., chest wall muscles) may be increasing their contribution to generating Pdi when the diaphragm force generating capacity is chronically compromised. A number of studies document a limited contribution of isolated chest wall muscles to breathing during cases of temporary or permanent diaphragm inactivation in both dogs and humans (Campbell, 1955; De Troyer et al., 2005; Legrand et al., 2003; Raper et al., 1966; Wilson et al., 2001). The specific contribution of chest wall muscles to Pdi is not well characterized in rats, and there are almost certainly species differences. For instance, in humans the bilateral maximal activation of all inspiratory related chest wall and neck (i.e., the sternocleidomastoid and scalene) muscles would cause a pressure change of only ~−25 cm H_2O (Legrand et al., 2003), which represents ~15% of Pdi_{max} in humans (Laporta et al., 1985). In agreement, humans with bilateral diaphragm muscle paralysis can generate pleural pressures of approximately −30 cm H_2O (~20% Pdi_{max}) against an occluded airway (Celli et al., 1987; Laroche et al., 1988). Conversely, in dogs, the bilateral maximal stimulation of inspiratory related chest wall and neck muscles would cause a pressure change of ~−15 cm H_2O (De Troyer et al., 2005; De Troyer et al., 1998a; De Troyer et al., 1998b), which represents ~25% of Pdi_{max} in dogs (De Troyer et al., 2003). If we extrapolate these data to rats, maximally activated inspiratory related chest wall muscles in rats would generate between ~6 and ~9 cm H_2O (~15% and ~25% of Pdi_{max}, respectively) (Gill et al., 2015; Mantilla et al., 2010). In the present study, Pdi during occlusion increased from 20 cm H_2O immediately after unilateral DNV to 27 cm H_2O 14 days later. Thus, it is possible that the bilateral maximal contraction of inspiratory related chest wall muscles including external and parasternal intercostal, scalene, sternocleidomastoid, and triangularis sterni muscles could be responsible for this additional pressure generation. As an initial approximation to investigate this possibility, the relative contributions of changes in Pes and Pga were analyzed as proposed by Macklem et al. (1978). The slope of the relationship between esophageal and gastric pressures for various behaviors generally reflects the relative contributions of chest wall inspiratory muscles and the diaphragm to Pdi. The average slope of this relationship

showed no significant difference over time after DNV. Importantly, analysis of the relative contributions of Pes and Pga is best suited for controlled conditions with human subjects, where particular pressures can be generated as requested by the investigators (Macklem et al., 1978). Under experimental conditions with anesthetized rats, the behaviors examined to evaluate varying levels of force generation using Pdi do not reflect controlled conditions for a single behavior with different levels of force. This may complicate interpretation of this technique in the present study. It is also worth noting that an overall increase in respiratory drive resulting in near-maximal contraction across multiple inspiratory related muscles was not reflected in the contralateral (intact) hemidiaphragm RMS_{75}. However, based on the findings of the current study, diaphragm EMG activity may not appropriately reflect changes in force production over time after DNV, possibly indicative of changes in the electromechanical coupling of the intact hemidiaphragm.

4.2. Effect of unilateral DNV on diaphragm EMG

The EMG time series is a spatially weighted sum of motor unit action potential trains (Basmajian et al., 1985). Previously, we showed a strong, linear correlation between diaphragm RMS_{peak} and Pdi across a range of motor behaviors ($r^2 = 0.78$) in intact rats (Mantilla et al., 2010). However, in the present study, changes in Pdi over time after DNV were not associated with concordant changes in diaphragm RMS_{peak} activity. The tension-time index was used as an estimate of the efficiency of diaphragm activation before, immediately after, and 14 days after DNV. Importantly, in the DNV group, the tension-time index increased after DNV and remained elevated above baseline after 14 days, consistent with an increased contribution of more fatigable motor unit types to force generation following inactivation of half of the motor unit pool after DNV. These findings suggest compensatory changes in the electromechanical coupling of the intact hemidiaphragm after DNV.

Increasing force in skeletal muscles can be accomplished by recruiting motor units and/or increasing the discharge frequency of recruited motor units (Mantilla et al., 2011b; Sieck, 1991; Sieck et al., 1989), neither of which is directly displayed in EMG. It is important to note that the level of synchrony in motor unit activation is directly related to the amplitude of the EMG signal (Yao et al., 2000). Discharge frequencies of motor units are modulated during motor behaviors as the level of activation increases (Seven et al., 2014), and this could occur in the intact hemidiaphragm after DNV. Importantly, increased recruitment of motor units or firing frequency only contribute to increased EMG amplitude when there is synchrony in motor unit activation and result in inconsistent effects if there is destructive interference between the multiple motor unit action potential trains. As a result, RMS EMG could remain relatively unchanged after DNV. In this regard, compound EMG recordings do not directly provide the necessary information to elucidate these possibilities, which may be elucidated by analysis of individual motor unit activity across many motor units. Unfortunately, these analyses are limited by the sampling of few motor units per hemidiaphragm and the inability to discriminate motor units as the level of force generation increases (Seven et al., 2014). The present results provide important, novel information about the restoration of Pdi during higher force motor behaviors over time after DNV.

5. Conclusion

Unilateral DNV removes all input from the ipsilateral hemidiaphragm. Since re-innervation does not occur within 14 days, all recovery can be attributed to compensatory mechanisms related neuroplasticity in respiratory motor control. As the primary inspiratory muscle, the diaphragm is the most likely candidate for changes in activity to occur after unilateral DNV. Future studies may use recently developed decomposition techniques for motor unit action potential recordings from multisite EMG electrodes in order to discriminate large numbers of motor units across a range of motor behaviors (De Luca et al., 2015; Nawab et al., 2010; Parsaei et al., 2010). Compensatory activation of inspiratory related chest wall and neck muscles may contribute to ameliorating the decreased Pdi during higher force behaviors after DNV. Examining the effect of unilateral diaphragm paralysis on an array of respiratory muscles – particularly the external and parasternal intercostal muscles bilaterally in conjunction with the diaphragm may be necessary to elucidate their relative contribution over time after DNV. Such studies could consider the differences in activation of intercostal muscles across thoracic segments that depend on position and that have been documented across species (De Troyer et al., 2005). The results of the present study suggest that compensatory changes in inspiratory muscles including the intact hemidiaphragm may emerge over time in conditions of unilateral paralysis.

Acknowledgments

This work was supported by National Institutes of Health (NIH) R01-HL096750, NIH HL105355 (T32), and the Mayo Clinic.

References

Alvarez-Argote S, Gransee HM, Mora JC, Stowe JM, Jorgenson AJ, Sieck GC, Mantilla CB. The Impact of Midcervical Contusion Injury on Diaphragm Muscle Function. J Neurotrauma. 2016; 33:500–509. [PubMed: 26413840]

Baltina TV, Eremeev AA, Pleshchinskii IN. The state of the contralateral neuromotor apparatus of the rat in conditions of unilateral tenotomy. Neurosci Behav Physiol. 2006; 36:385–389. [PubMed: 16583166]

Basmajian, JV., De Luca, CJ. Muscles alive: their functions revealed by electromyography. 5. Williams & Wilkins; Baltimore: 1985.

Bellemare F, Grassino A. Effect of pressure and timing of contraction on human diaphragm fatigue assessed by phrenic nerve stimulation. J Appl Physiol. 1982; 53:1190–1195. [PubMed: 7174413]

Campbell EJ. The role of the scalene and sternomastoid muscles in breathing in normal subjects; an electromyographic study. J Anat. 1955; 89:378–386. [PubMed: 13251968]

Celli BR, Rassulo J, Corral R. Ventilatory muscle dysfunction in patients with bilateral idiopathic diaphragmatic paralysis: reversal by intermittent external negative pressure ventilation. Am Rev Respir Dis. 1987; 136:1276–1278. [PubMed: 3674587]

De Luca CJ, Chang SS, Roy SH, Kline JC, Nawab SH. Decomposition of surface EMG signals from cyclic dynamic contractions. J Neurophysiol. 2015; 113:1941–1951. [PubMed: 25540220]

De Troyer A, Legrand A. Mechanical advantage of the canine triangularis sterni. J Appl Physiol (1985). 1998a; 84:562–568. [PubMed: 9475866]

De Troyer A, Legrand A, Gevenois PA, Wilson TA. Mechanical advantage of the human parasternal intercostal and triangularis sterni muscles. J Physiol. 1998b; 513(Pt 3):915–925. [PubMed: 9824728]

De Troyer A, Cappello M, Meurant N, Scillia P. Synergism between the canine left and right hemidiaphragms. J Appl Physiol (1985). 2003; 94:1757–1765. [PubMed: 12679346]

De Troyer A, Kirkwood PA, Wilson TA. Respiratory action of the intercostal muscles. Physiol Rev. 2005; 85:717–756. [PubMed: 15788709]

Dow DE, Mantilla CB, Zhan WZ, Sieck GC. EMG-based detection of inspiration in the rat diaphragm muscle. Conf Proc IEEE Eng Med Biol Soc. 2006; 1:1204–1207. [PubMed: 17946030]

Dow DE, Zhan WZ, Sieck GC, Mantilla CB. Correlation of respiratory activity of contralateral diaphragm muscles for evaluation of recovery following hemiparesis. Conf Proc IEEE Eng Med Biol Soc. 2009; 1:404–407.

Fournier M, Sieck GC. Mechanical properties of muscle units in the cat diaphragm. J Neurophysiol. 1988; 59:1055–1066. [PubMed: 3367195]

Geiger PC, Bailey JP, Zhan WZ, Mantilla CB, Sieck GC. Denervation-induced changes in myosin heavy chain expression in the rat diaphragm muscle. J Appl Physiol. 2003; 95:611–619. [PubMed: 12704093]

Gill LC, Mantilla CB, Sieck GC. Impact of unilateral denervation on transdiaphragmatic pressure. Respir Physiol Neurobiol. 2015; 210:14–21. [PubMed: 25641347]

Gosselin LE, Brice G, Carlson B, Prakash YS, Sieck GC. Changes in satellite cell mitotic activity during acute period of unilateral diaphragm denervation. J Appl Physiol. 1994; 77:1128–1134. [PubMed: 7836114]

Greising SM, Mantilla CB, Sieck DC, Sieck GC. Transdiaphragmatic pressure measurements reveal age-related diaphragm muscle dysfunction during non-ventilatory behaviors. FASEB J. 2013a:27.

Greising SM, Sieck DC, Sieck GC, Mantilla CB. Novel method for transdiaphragmatic pressure measurements in mice. Respir Physiol Neurobiol. 2013b; 188:56–59. [PubMed: 23632282]

Hart N, Nickol AH, Cramer D, Ward SP, Lofaso F, Pride NB, Moxham J, Polkey MI. Effect of severe isolated unilateral and bilateral diaphragm weakness on exercise performance. Am J Respir Crit Care Med. 2002; 165:1265–1270. [PubMed: 11991876]

Harvey PJ, Li Y, Li X, Bennett DJ. Persistent sodium currents and repetitive firing in motoneurons of the sacrocaudal spinal cord of adult rats. J Neurophysiol. 2006; 96:1141–1157. [PubMed: 16282206]

Hillman DR, Finucane KE. Respiratory pressure partitioning during quiet inspiration in unilateral and bilateral diaphragmatic weakness. Am Rev Respir Dis. 1988; 137:1401–1405. [PubMed: 3202378]

Iscoe S, Dankoff J, Migicovsky R, Polosa C. Recruitment and discharge frequency of phrenic motoneurones during inspiration. Respir Physiol. 1976; 26:113–128. [PubMed: 179122]

Katagiri M, Young RN, Platt RS, Kieser TM, Easton PA. Respiratory muscle compensation for unilateral or bilateral hemidiaphragm paralysis in awake canines. J Appl Physiol. 1994; 77:1972–1982. [PubMed: 7836225]

Krutki P, Haluszka A, Mrowczynski W, Gardiner PF, Celichowski J. Adaptations of motoneuron properties to chronic compensatory muscle overload. J Neurophysiol. 2015; 113:2769–2777. [PubMed: 25695651]

Laporta D, Grassino A. Assessment of transdiaphragmatic pressure in humans. J Appl Physiol. 1985; 58(5):1469–1476. [PubMed: 3158636]

Laroche CM, Carroll N, Moxham J, Green M. Clinical significance of severe isolated diaphragm weakness. Am Rev Respir Dis. 1988; 138:862–866. [PubMed: 3202460]

Legrand A, Schneider E, Gevenois PA, De Troyer A. Respiratory effects of the scalene and sternomastoid muscles in humans. J Appl Physiol (1985). 2003; 94:1467–1472. [PubMed: 12626472]

Liddell EGT, Sherrington CS. Recruitment and some other factors of reflex inhibition. Proc Roy Soc Lond (Biol). 1925; 97:488–518.

Lisboa C, Pare PD, Pertuze J, Contreras G, Moreno R, Guillemi S, Cruz E. Inspiratory muscle function in unilateral diaphragmatic paralysis. Am Rev Respir Dis. 1986; 134:488–492. [PubMed: 3752705]

Macklem PT, Gross D, Grassino GA, Roussos C. Partitioning of inspiratory pressure swings between diaphragm and intercostal/accessory muscles. J Appl Physiol Respir Environ Exerc Physiol. 1978; 44:200–208. [PubMed: 632159]

Mantilla CB, Seven YB, Zhan WZ, Sieck GC. Diaphragm motor unit recruitment in rats. Respir Physiol Neurobiol. 2010; 173:101–106. [PubMed: 20620243]

Mantilla CB, Seven YB, Hurtado-Palomino JN, Zhan WZ, Sieck GC. Chronic assessment of diaphragm muscle EMG activity across motor behaviors. Respir Physiol Neurobiol. 2011a; 177:176–182. [PubMed: 21414423]

Mantilla CB, Sieck GC. Phrenic motor unit recruitment during ventilatory and non-ventilatory behaviors. Respir Physiol Neurobiol. 2011b; 179:57–63. [PubMed: 21763470]

Mantilla CB, Seven YB, Sieck GC. Convergence of pattern generator outputs on a common mechanism of diaphragm motor unit recruitment. Prog Brain Res. 2014; 209:309–329. [PubMed: 24746055]

Medina-Martinez JS, Greising SM, Sieck GC, Mantilla CB. SemiAutomated Assessment of Transdiaphragmatic Pressure Variability across Motor Behaviors. Respiratory physiology & neurobiology. 2015

Miyata H, Zhan WZ, Prakash YS, Sieck GC. Myoneural interactions affect diaphragm muscle adaptations to inactivity. J Appl Physiol. 1995; 79:1640–1649. [PubMed: 8594024]

Nawab SH, Chang SS, De Luca CJ. High-yield decomposition of surface EMG signals. Clinical neurophysiology: official journal of the International Federation of Clinical Neurophysiology. 2010; 121:1602–1615. [PubMed: 20430694]

Parsaei H, Stashuk DW, Rasheed S, Farkas C, Hamilton-Wright A. Intramuscular EMG signal decomposition. Crit Rev Biomed Eng. 2010; 38:435–465. [PubMed: 21175408]

Rana S, Sieck GC, Mantilla CB. Diaphragm Electromyographic Activity following Unilateral Mid-Cervical Contusion Injury in Rats. J Neurophysiol. 2016 jn 00727 02016.

Raper AJ, Thompson WT Jr, Shapiro W, Patterson JL Jr. Scalene and sternomastoid muscle function. J Appl Physiol. 1966; 21:497–502. [PubMed: 5934453]

Seven YB, Mantilla CB, Sieck GC. Recruitment of Rat Diaphragm Motor Units Across Motor Behaviors with Different Levels of Diaphragm Activation. J Appl Physiol. 2014; 117:1308–1316. [PubMed: 25257864]

Sieck GC, Trelease RB, Harper RM. Sleep influences on diaphragmatic motor unit discharge. Exp Neurol. 1984; 85:316–335. [PubMed: 6745377]

Sieck GC. Diaphragm muscle: Structural and functional organization. Clin Chest Med. 1988; 9:195–210. [PubMed: 3292123]

Sieck GC, Fournier M. Diaphragm motor unit recruitment during ventilatory and nonventilatory behaviors. J Appl Physiol. 1989; 66:2539–2545. [PubMed: 2745316]

Sieck GC. Neural control of the inspiratory pump. NIPS. 1991; 6:260–264.

Sieck GC. Physiological effects of diaphragm muscle denervation and disuse. Clin Chest Med. 1994; 15:641–659. [PubMed: 7867280]

Thomas CK, Hager CK, Klein CS. Increases in human motoneuron excitability after cervical spinal cord injury depend on the level of injury. J Neurophysiol. 2016 jn 00676 02016.

Tissenbaum HA, Parry DJ. The effect of partial denervation of tibialis anterior muscle on the number and sizes of motoneurons in the motor nucleus of normal and dystrophic mice. Can J Physiol Pharmacol. 1991; 69:1769–1773. [PubMed: 1804521]

Trelease RB, Sieck GC, Harper RM. A new technique for acute and chronic recording of crural diaphragm EMG in cats. Electroencephalogr Clin Neurophysiol. 1982; 53:459–462. [PubMed: 6175508]

Watchko JF, Mayock DE, Standaert A, Woodrum DE. Postnatal changes in transdiaphragmatic pressure in piglets. Pediatr Res. 1986; 20:658–661. [PubMed: 3725464]

Wilson TA, Legrand A, Gevenois PA, De Troyer A. Respiratory effects of the external and internal intercostal muscles in humans. J Physiol. 2001; 530:319–330. [PubMed: 11208979]

Yao W, Fuglevand RJ, Enoka RM. Motor-unit synchronization increases EMG amplitude and decreases force steadiness of simulated contractions. J Neurophysiol. 2000; 83:441–452. [PubMed: 10634886]

Zhan WZ, Sieck GC. Adaptations of diaphragm and medial gastrocnemius muscles to inactivity. J Appl Physiol. 1992; 72:1445–1453. [PubMed: 1592737]

Zhan WZ, Farkas GA, Schroeder MA, Gosselin LE, Sieck GC. Regional adaptations of rabbit diaphragm muscle fibers to unilateral denervation. J Appl Physiol. 1995; 79:941–950. [PubMed: 8567538]

Zhan WZ, Miyata H, Prakash YS, Sieck GC. Metabolic and phenotypic adaptations of diaphragm muscle fibers with inactivation. J Appl Physiol. 1997; 82:1145–1153. [PubMed: 9104851]

Highlights

- Simultaneous Pdi and diaphragm EMG measurements provide information about neuroplasticity in motor control after chronic unilateral diaphragm denervation (DNV).
- Pdi amplitude during ventilatory behaviors was unimpaired, but inspiratory duration and duty cycle increased immediately after DNV before returning to baseline 14 days later.
- A ~45% decrease in Pdi amplitude during airway occlusion immediately after DNV was ameliorated to ~25% by 14 days later.
- Compensatory activation of inspiratory related muscles other than the diaphragm may account for increased Pdi during higher force behaviors over time.

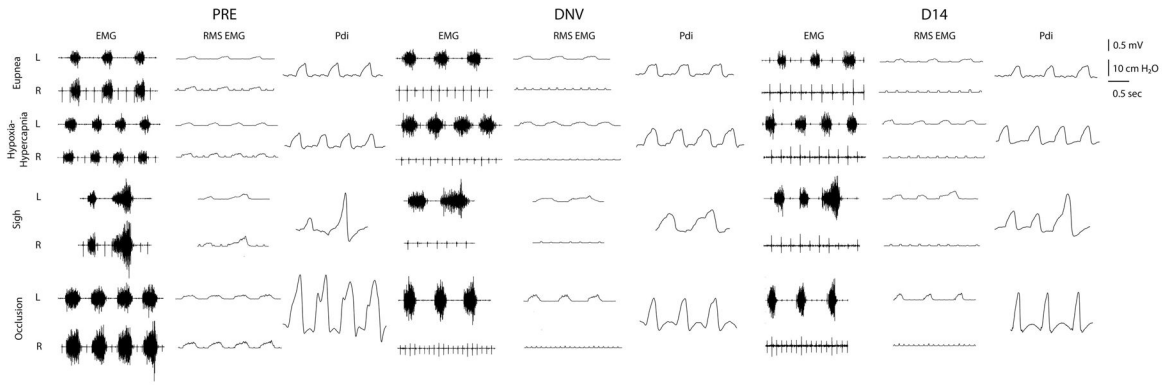

Figure 1.

Representative bilateral (L, left; R, right) tracings from a single animal in the denervation group displaying compound diaphragm EMG, root mean square (RMS) EMG, and transdiaphragmatic pressure (Pdi) at baseline (PRE), immediately after unilateral denervation (DNV), and 14 days afterwards (D14) across eupnea, hypoxia-hypercapnia (10% O_2–5% CO_2), spontaneous deep breaths (sighs), and airway occlusion. Pdi during higher force behaviors showed a significant decrease immediately after denervation and partial recovery by 14 days. Note diaphragm activity in bursts across behaviors and complete absence of ipsilateral activity after denervation (DNV and D14). ECG artifact is visible in the EMG tracings. The scale bars represent voltage (in mV for the EMG and RMS EMG signals), pressure (in cmH_2O for Pdi) and time (in s for all signals).

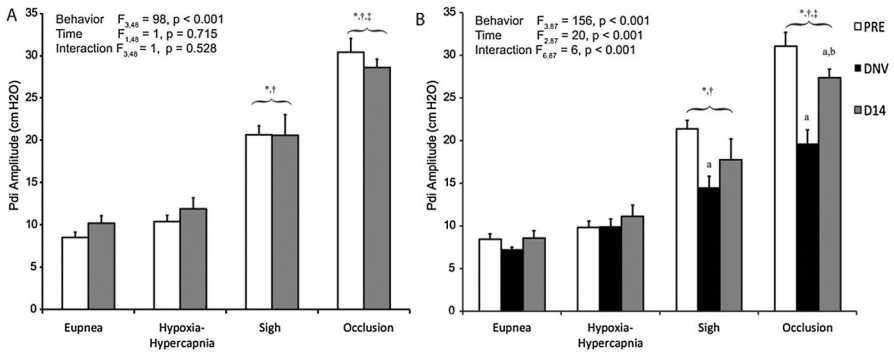

Figure 2.

Pdi amplitude (mean ± SE) during ventilatory and higher force, non-ventilatory behaviors at baseline (PRE, white bars), after unilateral denervation (DNV, black bars), and 14 days after baseline (D14, gray bars) in control (A, n = 8; n=6 for sigh) and denervation groups (B, n = 9; n = 8 for sigh). Main effects from the mixed linear model are presented in the text box and pairwise comparisons denoted by the significance symbols. As expected, Pdi amplitude during sigh and occlusion is higher than for hypoxia-hypercapnia and eupnea in both groups at all time-points. There were no differences over time in the control group (see 3.1). In the denervation group, Pdi amplitude during sigh and airway occlusion was significantly reduced immediately after unilateral denervation, but only during airway occlusion by 14 days afterwards. *, different from eupnea for the same time-point ($p < 0.05$); †, different from hypoxia-hypercapnia for the same time-point ($p < 0.\ 05$); ‡, different from sigh for the same time-point; [a], different from PRE for the same motor behavior ($p < 0.05$); [b], different from DNV for the same motor behavior ($p < 0.05$).

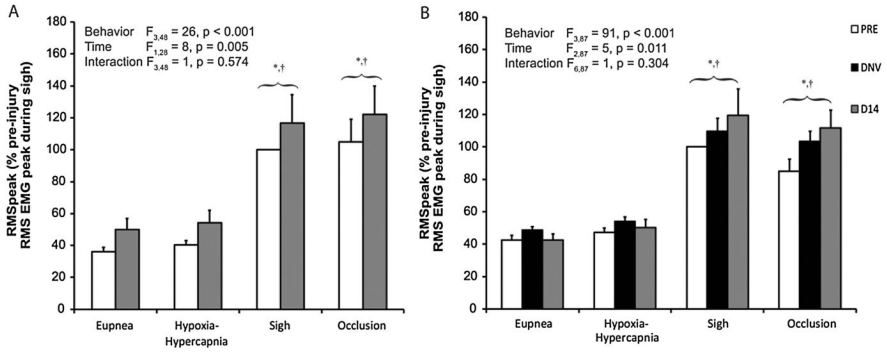

Figure 3.

Peak RMS EMG (normalized to the peak RMS EMG during sigh at baseline; RMS_{peak}) during ventilatory and higher force, non-ventilatory behaviors at baseline (PRE, white bars), after unilateral denervation (DNV, black bars), and 14 days after baseline (D14, gray bars) in control (A, n = 8; n=6 for sigh) and denervation groups (B, n = 9; n = 8 for sigh). Main effects from the mixed linear model are presented in the text box and pairwise comparisons denoted by the significance symbols. As expected, RMS_{peak} during sigh and occlusion is higher than for hypoxia-hypercapnia and eupnea in both groups at all time-points. There was a significant effect of time on RMS_{peak} in both groups, but no effect of denervation (see 3.2). *, different from eupnea for the same time-point ($p < 0.05$); †, different from hypoxia-hypercapnia for the same time-point ($p < 0.05$).

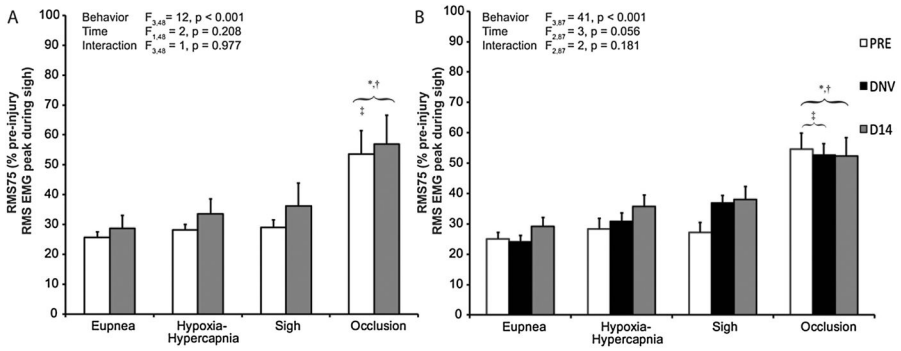

Figure 4.

Neural drive to phrenic motoneurons (central respiratory drive) estimated by the RMS EMG value at 75 ms after onset (normalized to peak RMS EMG during sigh at baseline; RMS_{75}). RMS_{75} is shown across motor behaviors at baseline (PRE, white bars), after unilateral denervation (DNV, black bars), and 14 days after baseline (D14, gray bars) in control (A, n = 8; n=6 for sigh) and denervation groups (B, n = 9; n = 8 for sigh). Main effects from the mixed linear model are presented in the text box and pairwise comparisons denoted by the significance symbols. As expected, RMS_{75} during occlusion was significantly greater than RMS_{75} during eupnea, hypoxia-hypercapnia, and sigh. There was no statistically significant effect on RMS_{75} as a result of chronic denervation (see 3.3). *, different from eupnea for the same time-point ($p < 0.05$); †, different from hypoxia-hypercapnia for the same time-point ($p < 0.05$); ‡, different from sigh for the same time-point ($p < 0.05$).

Table 1

Ventilatory parameters across motor behaviors in control (n = 8) and denervation (n = 9) rats.

	Eupnea			Hypoxia-Hypercapnia		
	PRE	**DNV**	**D14**	**PRE**	**DNV**	**D14**
Respiratory Rate (min^{-1}) *,†						
Control	58 ± 3		58 ± 3	78 ± 4		75 ± 3
Denervation	60 ± 3	59 ± 2	67 ± 3	77 ± 3	72 ± 3	85 ± 5
Inspiratory Duration (ms) †,‡						
Control	288 ± 11		276 ± 17	277 ± 11		260 ± 14
Denervation	287 ± 10	360 ± 15	262 ± 11	285 ± 14	355 ± 14	258 ± 11
Duty Cycle (%) *,†,‡						
Control	27 ± 1		27 ± 1	36 ± 1		32 ± 3
Denervation	29 ± 1	33 ± 2	29 ± 1	37 ± 2	41 ± 2	38 ± 1
Tension-Time Index (%) *,†,‡						
Control	7.1 ± 0.9		8.4 ± 1.0	11.3 ± 1.7		12.7 ± 2.4
Denervation	7.3 ± 1.0	11.2 ± 1.1	11.7 ± 1.8	10.5 ± 1.2	20.0 ± 3.0	18.9 ± 2.7

*, significant effect of behavior in control group;

†, significant effect of behaviors in denervation group;

‡, significant effect of time in denervation group